

Shake table responses of an RC low-rise building model strengthened with buckling restrained braces at ground story

Han Seon Lee^{*1}, Kyung Bo Lee¹, Kyung Ran Hwang¹ and Chang Seok Cho²

¹*School of Civil, Environmental, and Architectural Engineering, Korea University, Seoul 136-713, Korea*

²*WISE Structural Engineering Co. Ltd, Seoul, 137-071, Korea*

(Received January 8, 2013, Revised September 30, 2013, Accepted October 26, 2013)

Abstract. In order to verify the applicability of buckling restrained braces (BRB's) and fiber reinforced polymer (FRP) sheets to the seismic strengthening of a low-rise RC building having the irregularities of a soft/weak story and torsion at the ground story, a series of earthquake simulation tests were conducted on a 1:5 scale RC building model before, and after, the strengthening, and these test results are compared and analyzed, to check the effectiveness of the strengthening. Based on the investigations, the following conclusions are made: (1) The BRB's revealed significant slips at the joint with the existing RC beam, up-lifts of columns from RC foundations and displacements due to the flexibility of foundations, and final failure due to the buckling and fracture of base joint angles. The lateral stiffness appeared to be, thereby, as low as one seventh of the intended value, which led to a large yield displacement and, therefore, the BRB's could not dissipate seismic input energy as desired within the range of anticipated displacements. (2) Although the strengthened model did not behave as desired, great enhancement in earthquake resistance was achieved through an approximate 50% increase in the lateral resistance of the wall, due to the axial constraint by the peripheral BRB frames. Finally, (3) whereas in the original model, base torsion was resisted by both the inner core walls and the peripheral frames, the strengthened model resisted most of the base torsion with the peripheral frames, after yielding of the inner core walls, and represented dual values of torsion stiffness, depending on the yielding of core walls.

Keywords: reinforced concrete; irregular; earthquake simulation test; torsion; buckling-restrained brace

1. Introduction

Many low-rise residential apartment buildings have recently been constructed in densely populated areas of Korea. As a result of the lack of available sites, the ground floor is usually used for a parking space, and adopts a piloti story. This type of building, as shown in Fig. 1(a), commonly has a high degree of irregularity of soft story, weak story, and torsion at the ground story. Observations of the damages to these structures imposed by severe earthquakes, such as the 1995 Kobe (Fukuta *et al.* 2001) and 2008 Sichuan earthquakes (Zhao *et al.* 2008), have drawn the conclusion that this type of building structure is vulnerable to severe damage, or complete collapse of the ground story. A large number of these buildings have been constructed in Korea, without

^{*}Corresponding author, Professor, E-mail: hslee@korea.ac.kr

considering the earthquake resistant design requirements. However, the Korean Building Code (KBC) 2005 (Architectural Institute of Korea 2005), which basically follows the framework of the International Building Code (IBC) 2000 (International Code Council 2000) with some minor modifications, together with other related building laws, enforces the seismic strengthening of these existing building structures. Strengthening existing building structures has been one of the main research topics, worldwide, since the 1990's.

One of the strengthening approaches for this type of structure is as follows; The ground story is strengthened in columns with fiber reinforced polymer (FRP) sheets, to prevent brittle collapse due to shear failure, and the peripheral frames at the ground story are infilled with buckling-restrained braces (BRB's), to reduce the degree of irregularity regarding the soft/weak story and torsion, and to increase the energy dissipation within the allowed range of drifts.

A study on the design of BRB components was presented by Chen (2002). The application of BRB's to a steel structure (Tremblay *et al.* 1999, Erochko *et al.* 2011) and displacement based seismic design approach for the use of BRB's (Teran-Gilmore *et al.* 2009) were studied. A design approach regarding the connection of BRB's to the steel structure was developed through experiment and analysis by Chou and Chen (2009), Chou and Liu (2012), and Chou *et al.* (2012). Recently, application of BRB's to an existing RC frame led to stable energy dissipation without a joint problem (Khampanit *et al.* 2011). However, in this experiment, the upper beam and the bottom footing connected to K-shaped BRB's in the one-bay one-story subassembly were so massive, that the connection details of the test specimen do not represent the realistic situation of existing RC frames.

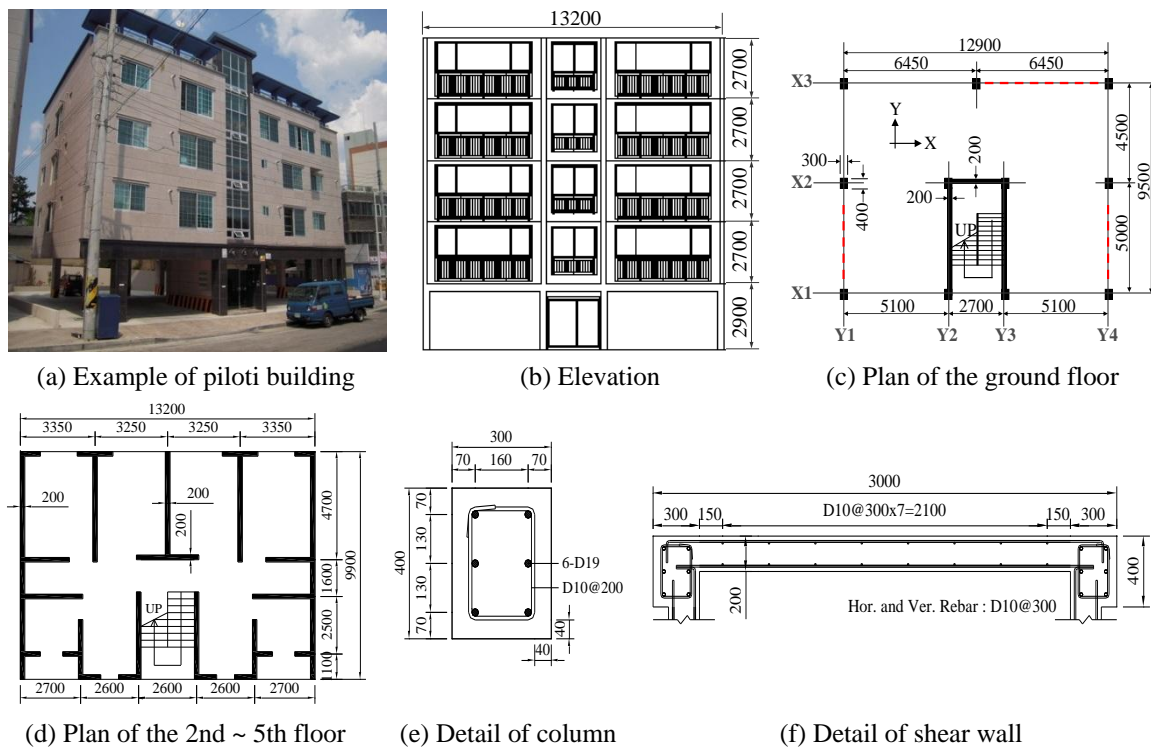


Fig. 1 Prototype structure (unit: mm)

The objective of the study stated herein is to verify applicability of BRB's and FRP sheets to seismic strengthening of a low-rise RC building having the irregularities of a soft/weak story and torsion at the ground story. The study deals with only one building model. So, the findings made thereby may not be generalized; but can provide some insight, particularly into the use of BRB's for seismically irregular RC buildings in low-to-moderate seismicity regions, such as Korea.

2. Design of the model and experimental setup

2.1 Design of the original model

Dimensions and details of the 5-story RC prototype are shown in Figs. 1 (b) to (f). The lowest two stories of the 1:5 scale structure model was designed and constructed to strictly satisfy the similitude requirements, while the upper three stories was replaced by concrete blocks of similar volume as shown in Fig. 2. This modified model enabled the reduction of time and cost for construction, without significant loss of similitude in the response. The total mass of the model is estimated to be 265.9kN, which is 7% less than the 285.9kN required by similitude for a true replica model. The model reinforcements, D4 and D2, representing the D19 and D10 reinforcements with the nominal yield strength of 400MPa in the prototype, were made by deforming wires. Heat treatment was conducted on these model reinforcements to ensure the target yield forces (D4: 4.4kN, D2: 1.1kN) in accordance with the similitude requirements. The achieved average yield forces of model reinforcements, D4 and D2, were 4.56kN and 1.3kN, respectively. The average compressive strength of the model concrete obtained from 28-day compression cylinder tests was 30.2MPa with the design strength of 21MPa. Detailed information of the original design and construction of the model is presented in Lee *et al.* (2011a).

The first series of earthquake simulation tests of the original model without strengthening were conducted up to the level of design earthquake (DE) in Korea, in 2009 at the Korea Institute of Machinery and Materials (KIMM), as shown in Fig. 3 (Lee *et al.* 2011a).

2.2 Design of the model strengthened with BRB's and FRP sheets

To complement the irregularity of the original model, i.e. soft story, weak story, and torsional

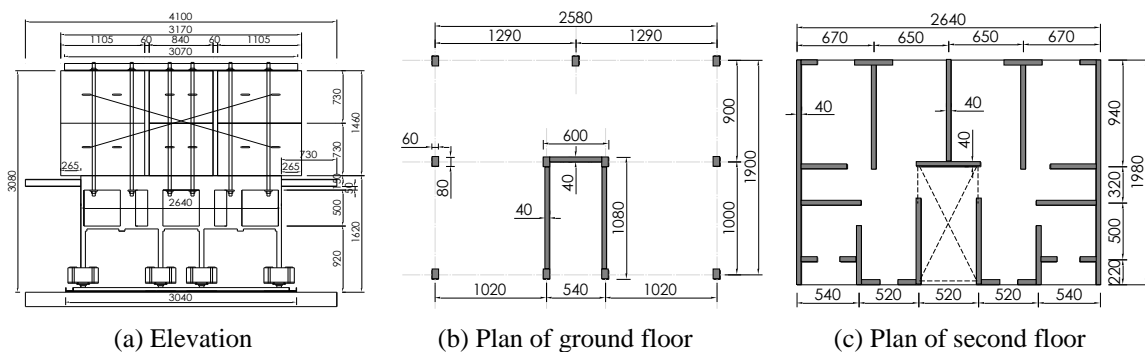


Fig. 2 Dimension of 1:5 scale model (unit: mm)



Fig. 3 Overview of earthquake simulation test set-up of the original model

eccentricity, the prototype was strengthened by BRB's and FRP sheets in the peripheral frames, as shown in Fig. 4. Evaluations of the original prototype regarding the irregularities, in accordance with KBC 2005, are given in Table 1. The strength, stiffness, and torsional irregularity of the original building appear to be very high. Detailed designs of BRB's and FRP sheets are given below. However, even with this strengthening, since the degrees of irregularity were so high in the original design, the resulting strengthened building still does not satisfy the requirement for regularity. The stiffness and strength of the strengthened first story are slightly increased when compared to those of the second story, because the ratio of the wall area to the floor area, 10.5%, is much larger than that at the first story 1.93%. However, the strengthened model alleviates the degree of irregularity for the torsion irregularity in the Y- direction, as shown in Table 1.

The design of the BRB's was conducted by following the procedure proposed by Chen (2002). The Y1 frame in Fig. 4 is assumed to resist a lateral load of 740kN ($2V_L$), which is about 20% of

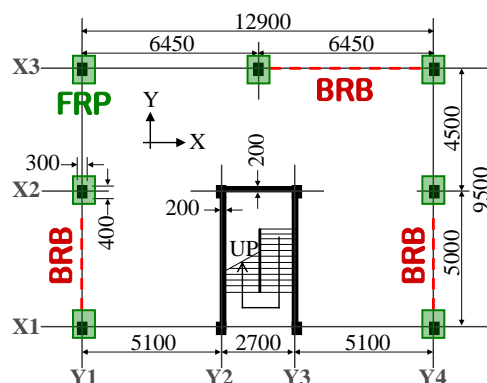


Fig. 4 Plan of strengthening with BRB's and FRP sheets at ground floor

Table 1 Assessment of irregularity at ground story according to KBC2005

| Irregularity | Criteria | Original | | Strengthened | |
|--------------|----------------------------------|----------|--------|--------------|--------|
| | | X-dir. | Y-dir. | X-dir. | Y-dir. |
| Stiffness | If $K_1/K_2 < 0.7$, | 0.159 | 0.160 | 0.218 | 0.213 |
| | irregular (NG) | (NG) | (NG) | (NG) | (NG) |
| Strength | If $F_1/F_2 < 0.8$, | 0.181 | 0.284 | 0.260 | 0.356 |
| | irregular (NG) | (NG) | (NG) | (NG) | (NG) |
| Torsion | If $\delta_{max}/\delta_{avg} >$ | 1.18 | 1.82 | 1.26 | 1.31 |
| | 1.2, irregular (NG) | (OK) | (NG) | (NG) | (NG) |

K_1/K_2 : Stiffness of first story / stiffness of second story

F_1/F_2 : Strength of first story / strength of second story

$\delta_{max}/\delta_{avg}$: Maximum / average drift

the level of the elastic base shear (base shear / effective weight of the structure (V/W) = 0.528 = 3,774kN/7,148kN) according to KBC 2005. The section area of the core plate is calculated by using Eq. (1), with the yield strength of the core plate being 375MPa. The lateral stiffness (K_L), and the yield displacement (δ_y) of the BRB's, excluding the RC frame, are calculated by using Eqs. (2) and (3), respectively, with the details of the BRB as shown in Fig. 5 (a) and the configuration of BRB's infilled in the frame as shown in Fig. 5 (b).

$$A_c = \frac{V_L}{F_y \cos \theta} = \frac{740kN / 2}{357(MPa) \cos 49^\circ} = 1,600mm^2 \quad (1)$$

$$K_L = \frac{E \cos^2 \theta}{\gamma + \eta(1 - \gamma)} \times \frac{2A_c}{L} = 125.4kN/mm \quad \left(\gamma = \frac{L_c}{L} = \frac{1600}{3400} = 0.47, \eta = \frac{A_c}{A_{p \text{ int}}} = \frac{1600}{4600} = 0.348 \right) \quad (2)$$

$$\delta_y = \frac{2V_L}{K_L} = \frac{740kN}{125.4kN/mm} = 5.9mm \quad (3)$$

where, A_c : core area (mm^2), V_L : applied lateral force to one BRB (kN), F_y : yield strength of the core (MPa), θ : angle of brace (49°), K_L : stiffness of the brace (kN/mm), L_c : core length of the brace (mm), L : total length of the brace (mm), η : ratio of the average axial stress in the brace outside the brace core to the stress in the brace core, δ_y : yield displacement of the brace (mm), E : modulus of elasticity of core steel (MPa).

In Fig. 6, the strength and stiffness of each frame and wall before, and after, strengthening are schematically compared. The yield strength of each frame is defined by the nominal lateral strength of the column and the wall, and the stiffness of each frame is obtained from an elastic analysis using the commercial finite element software, DIANA 9.1 (De Witte and Kikstra, 2005). Fig. 6(b) shows that the stiffness and strength of the strengthened frames are greatly increased compared to those of the original frames. Particularly, the values of stiffness of the strengthened frames in X and Y directions are approximately 9.5 and 5 times larger than those of the original frames, respectively. However, the values of stiffness of the strengthened frames in the X and Y

directions are as low as a half and a quarter of those of the walls, respectively. The strength of each frame and wall is the sum of the nominal lateral strength of the columns, BRB's, and the walls, and the stiffness of each frame and wall was obtained by elastic analysis.

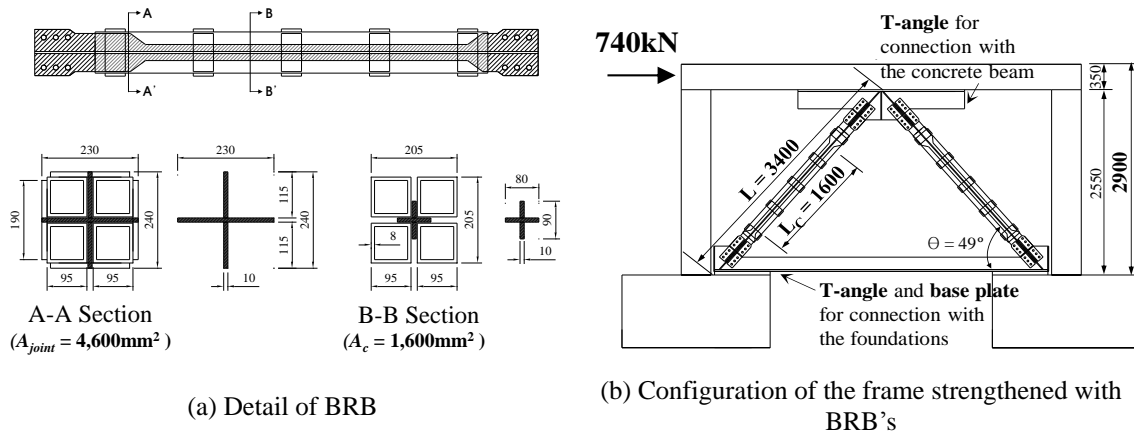


Fig. 5 Design of the prototype BRB's (unit: mm)

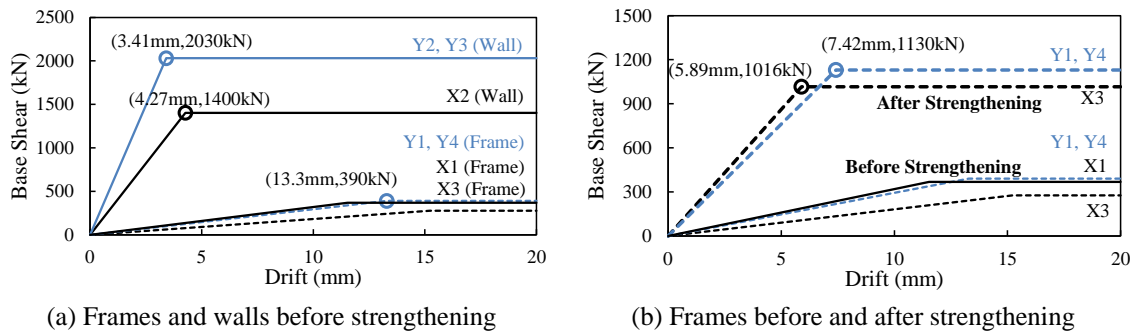


Fig. 6 Schematic comparison of strength and stiffness of frames and walls of the prototype (See Fig. 4 for definition of the frames and walls, X1, X2, X3, Y1, Y2, Y3, and Y4)

Columns at the peripheral frames are strengthened with double-layered FRP sheets, to enhance the shear and axial strength to prevent brittle failure due to shear failure, followed by axial compressive failure under seismic load. The properties of the FRP are shown in Table 2. The shear strengths of the column strengthened with FRP sheets are estimated by summing V_n and V_{frp} , calculated using Eqs. (4) and (5), respectively (Teng *et al.* 2002, Sheikh and Li 2007).

$$V_n = V_c + V_s = \frac{1}{6} \sqrt{f_c'} b_w d + \frac{A_v f_y d}{s} = 128 \text{ kN (X-dir.)}, 156 \text{ kN (Y-dir.)} \quad (4)$$

$$V_{frp} = 2 f_{frp,e} t_{frp} d' \cot \theta = 269 \text{ kN (X-dir.)}, 358 \text{ kN (Y-dir.)} \quad (5)$$

where, V_n : nominal shear strength according to ACI 318-05 (V_c =concrete shear, V_s =steel shear), f'_c : the compressive strength of the concrete, b_w : web width of section, d : distance from extreme compression fiber to centroid of longitudinal tension reinforcement, A_v : the cross-sectional area of the hoop, f_y : the yield strength of the hoop (400MPa), s : the spacing of the hoop (200mm), θ : the inclination of the critical shear crack to the column axis (35°), V_{frp} : nominal shear strength of FRP, $f_{frp,e}$: the tensile stress limit of the FRP, t_{frp} : the thickness of the FRP jacket, and d' : the section depth in the lateral load direction.

Table 3 compares the shear and axial strength of the columns before, and after, strengthening. The nominal shear strength in the main body of the strengthened column is over three times larger than the original, and the nominal axial strength of the strengthened model also increased by 27%, when compared to that of the original. In spite of the increase of axial and shear strength in the main body of columns, the lateral strength will be controlled by the yield strength at the joint between the beam and column, or between the column and foundation where the FRP sheets do not have any strengthening effect. The lateral strength corresponding to the plastic hinging at both top and bottom of the columns are shown as V_p in Table 3. Therefore, the increase in the lateral strength of the frame by using FRP sheets is not effective, due to the plastic hinging at the top and bottom joints of columns. However, brittle shear failure followed by axial failure in the main body of columns can be prevented by using FRP sheets.

2.3 Static lateral load test on 1:5 scale subassemblages strengthened with BRB's and FRP sheets

To verify the performance of the frames strengthened with the BRB's and FRP sheets, the lateral load tests of strengthened subassemblages (LC1 and LC2) were carried out as shown in Fig. 7 (Lee *et al.* 2011b). Specimen LC1 has one load cell below each footing to measure the base shear and axial forces, which has the same condition as in the earthquake simulation test, while specimen LC2 has two load cells. In Table 4 and Fig. 8, the yield strength of specimen LC1 is similar to the design strength, but the value of initial stiffness is significantly lower than that of design, due to the

Table 2 Property of the FRP sheets

| Elastic Modulus (GPa) | Strain limit (Elastic) | Tensile stress limit ($f_{frp,e}$, MPa) | Thickness (t_{frp} , mm) |
|-----------------------|------------------------|---|-----------------------------|
| 235 | 0.004 | 940 | 0.167 |

Table 3 Comparison of the shear and axial strength capacity of columns before and after FRP strengthening (unit: kN)

| Nominal strength | Before strengthening | | After strengthening | |
|------------------|----------------------|--------|---------------------|--------|
| | X-dir. | Y-dir. | X-dir. | Y-dir. |
| V_n | 128 | 156 | 397 | 514 |
| V_p^{**} | 92 | 130 | - | - |
| P_n | 2,235 | | 2,830 | |

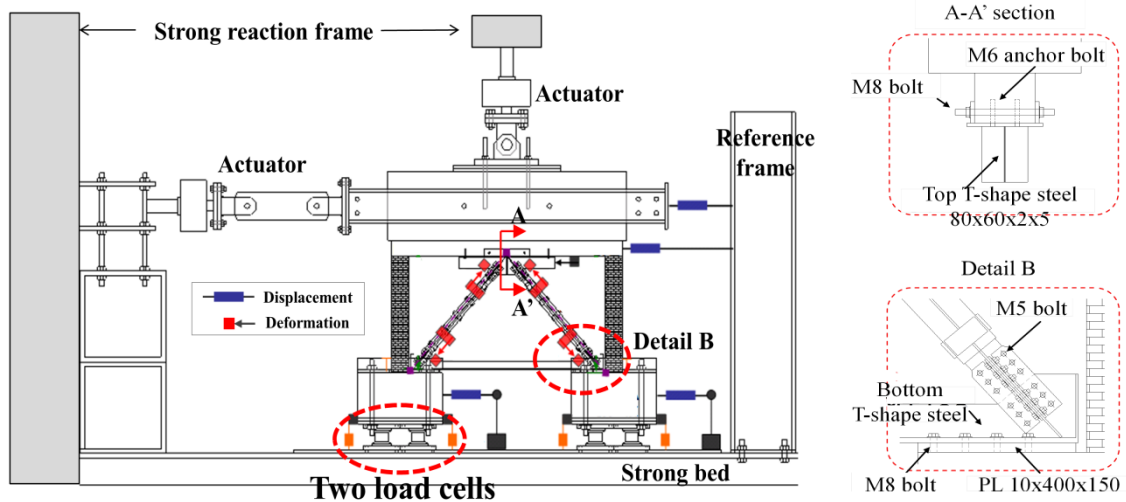
* Strength reduction factors were not applied to compute all of the above capacities.

** Shear capacity by plastic hinging at the top and bottom ends of the column.

flexibility of the footing. Though the strength and stiffness of specimen LC2 is significantly larger than those of specimen LC1, the lateral stiffness of specimen LC2 is still lower than the design value. The drift of LC2 is composed of the actual lateral drift of frame, slippage of upper and lower connections of BRB's, and lateral drift due to the flexibility of the footing, as shown in Fig. 9 (e). The stiffness of LC2 considering only this actual lateral drift of frame (Mod_LC2) is similar to that of the design in Table 4. The main failure modes of specimen LC2 are joint failure at the top of columns, up-lifts at the joints of column bases, and buckling of T angles at the bottom joints of BRB's, as shown in Fig. 10.



(a) Overview of test setup



(b) Details of specimen

Fig. 7 Lateral load test setup of 1:5 scale sub-assemblages strengthened with BRB's and FRP (Specimen LC2)

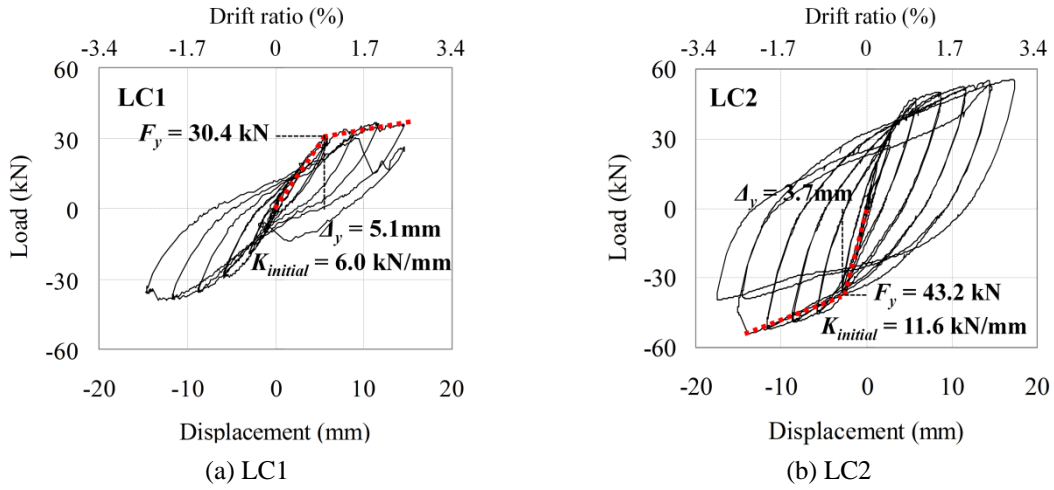


Fig. 8 Force-displacement relation of subassemblages (LC1, LC2)

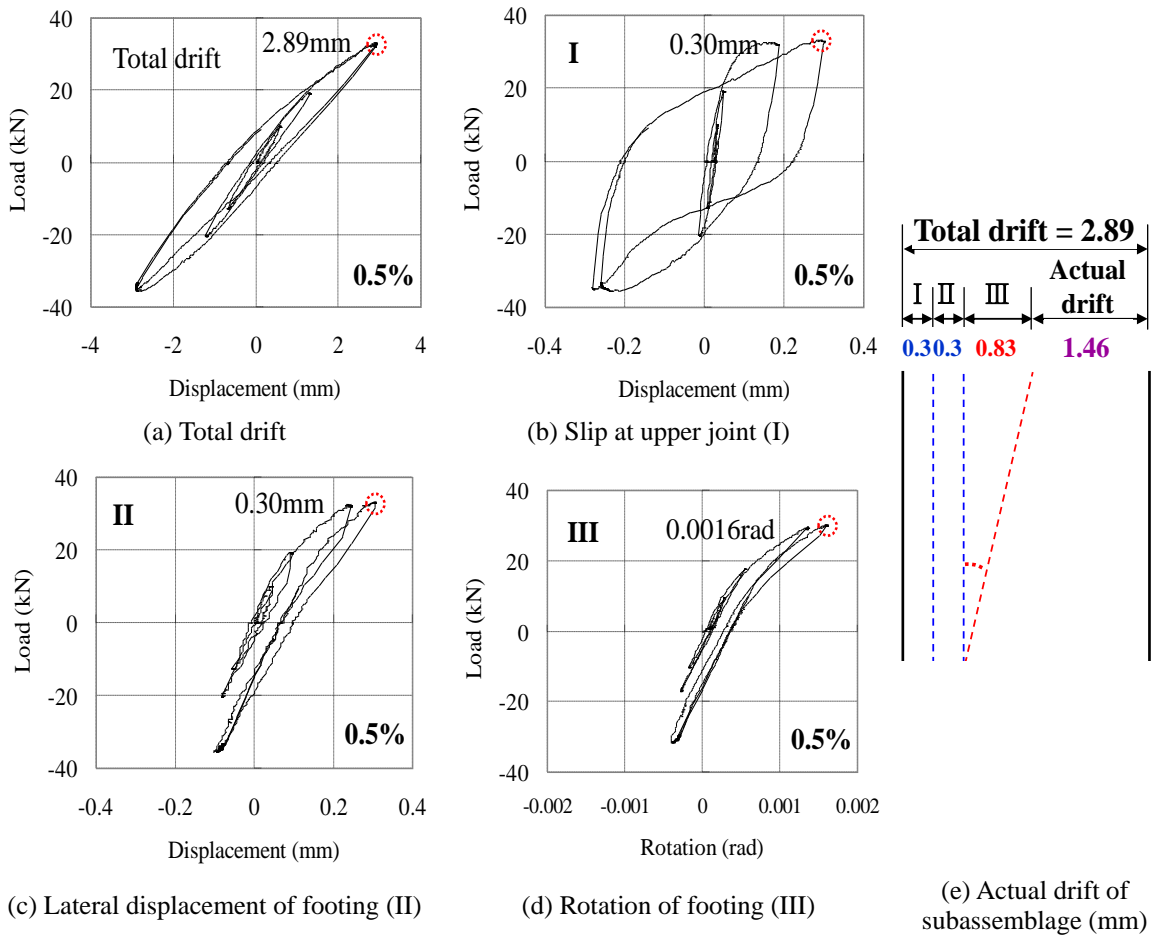


Fig. 9 Composition of displacement of LC2 at 0.5% drift ratio

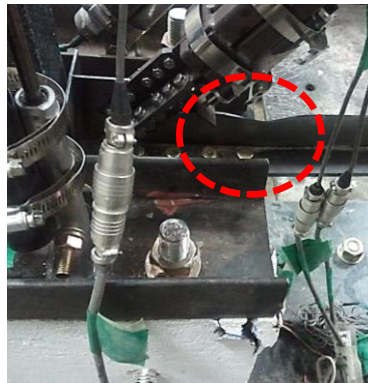
Table 4 Yield strength and lateral stiffness of 1:5 scale subassemblages strengthened with BRB's and FRP

| Specimens | Yield drift (mm) | Yield strength (kN) | Stiffness (kN/mm) |
|--------------|------------------|---------------------|-------------------|
| Design value | 1.2 | 30 | 25.1 |
| Static test | | | |
| LC1* | 5.1 | 30.4 | 6.0 |
| LC2 | 3.7 | 43.2 | 11.6 |
| Mod_LC2 | 1.9 | 43.2 | 22.6 |

* Identical condition to the earthquake simulation test



(a) Failure of joint at the top of column



(b) Buckling of T angle



(c) Uplift of column and buckling of T angle

Fig. 10 Failure modes of LC2 (view after elimination of base plate)

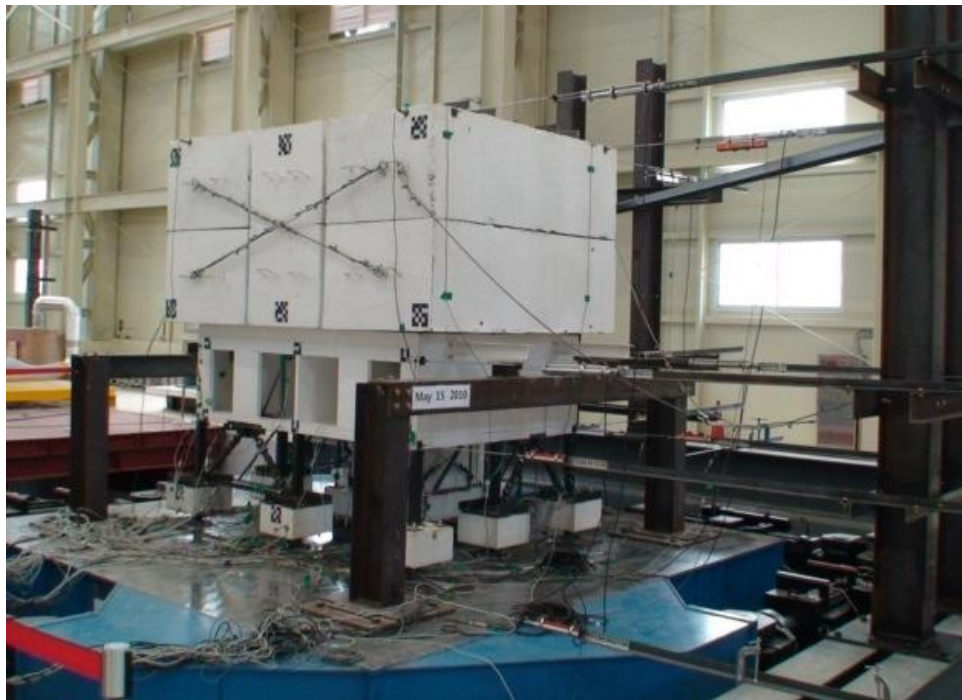


Fig. 11 Overview of earthquake simulation test set up of the model strengthened with BRB's and FRP

2.4 Experimental setup of earthquake simulation tests

A series of earthquake simulation tests of the strengthened model was carried out at the Seismic Simulation Test Center at Pusan National University, Korea, in 2010 (Fig. 11). The experimental set-up and instrumentation to measure the displacements, accelerations, and forces are shown in Fig. 12. The instrumentation and experimental setup are similar to the first series of earthquake simulation tests, as shown in Fig. 3 (Lee *et al.* 2011a).

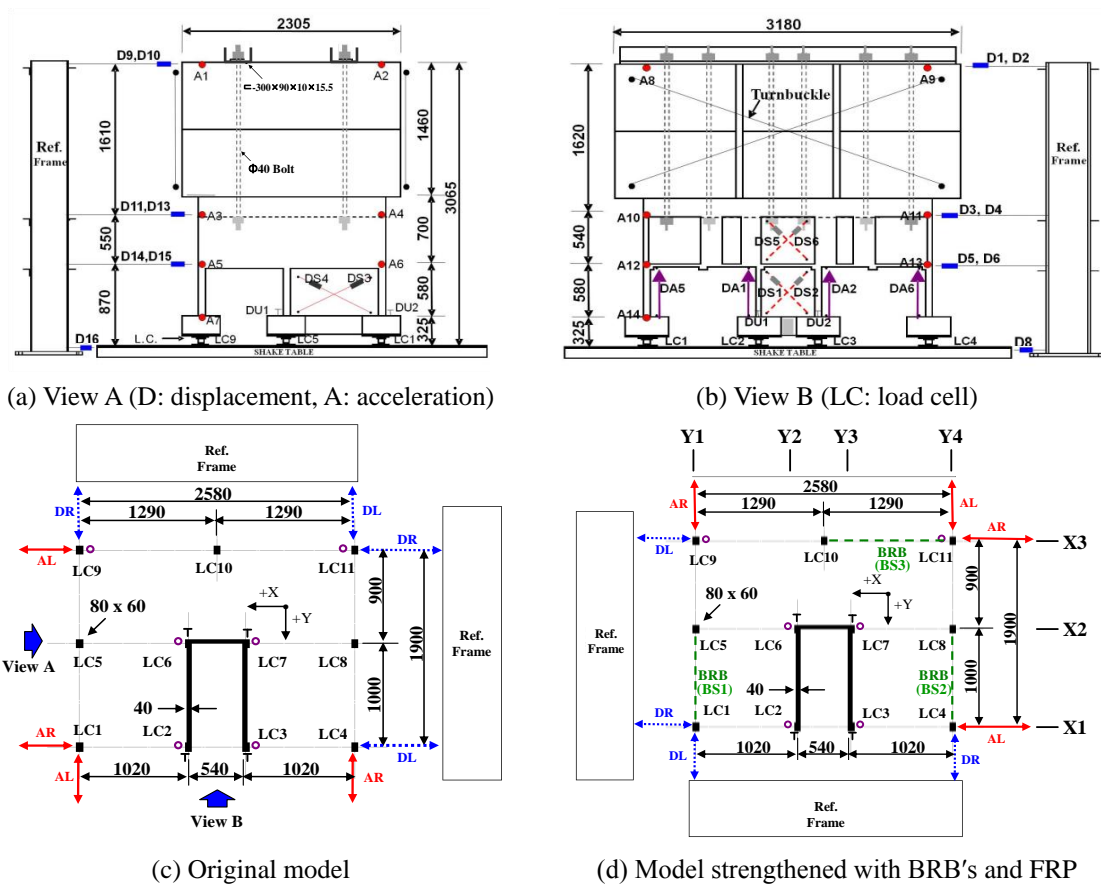


Fig. 12 Dimensions and instrumentation of the 1:5 scale structure model

3. Comparison of results of earthquake simulation tests before and after strengthening

3.1 Test program

The program of earthquake simulation tests before, and after, strengthening is summarized in Table 5. The target or input accelerogram of the table was based on the recorded 1952 Taft N21E (X direction) and Taft S69E (Y direction) components, and was formulated by compressing the

time axis with a scale factor of $1/\sqrt{5}$, and by adjusting the peak ground acceleration (PGA) to match the corresponding (KBC2005) elastic design spectrum. The designation and significance of each earthquake simulation test is given in the table. First, the test was performed with the table excitations in only one direction (X direction), and the consecutive test was conducted in the two orthogonal directions (X and Y directions), for each level of earthquake intensity. Detailed information on the results of earthquake simulation tests on the original model is presented in Lee *et al.* (2011a). Whereas the original model was subjected only to the level of design earthquake (DE), the strengthened model was tested not only up to the levels of maximum considered earthquake (MCE) in Korea, but also to the level of design earthquake in San Francisco. The designations for the tests of the strengthened model include R as the first character. The paper deals mainly with the effect of strengthening, by comparing the test results of the strengthened model with those of the original.

3.2 Design spectra and experiment results

Elastic response spectra are given in Fig. 13 (a) for DE, MCE, and shake-table input and output. Generally, the shake-table outputs simulated well the DE and MCE, except the case of DE for the original model (0.187XY). The measured PGA's for each test are compared with the intended, in Table 6. Since the output of 0.154XY appear to be similar to the input of 0.187XY intended for the design earthquake, and the response spectra of the output of 0.154XY in Fig. 13 (a) generally simulate the design spectrum, the response of the original model under test 0.154XY is assumed to represent the response to the design earthquake.

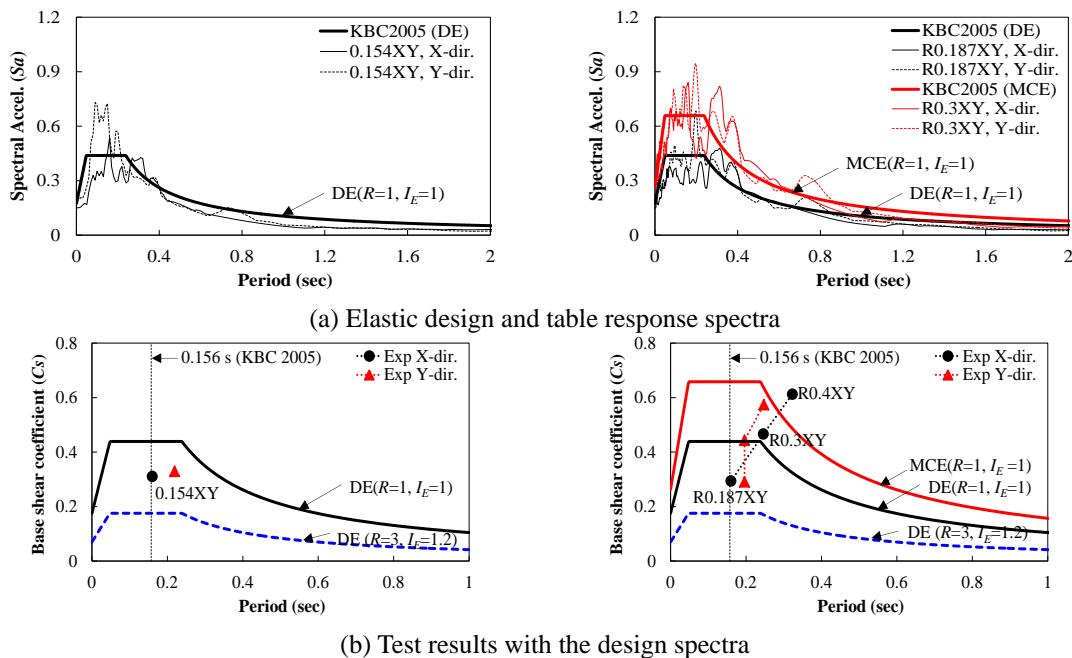


Fig. 13 Comparison with elastic design spectra of DE and MCE and table output response spectra (R : the response modification factor and I_E : the importance factor)

Fig. 13 (b) compares elastic design spectra corresponding to the DE and the MCE with the seismic response (or base shear) coefficients, C_S = the base shear / the effective seismic weight = V/W , derived from the maximum base shear in the each test result. The values of seismic response coefficients of the original model under DE (0.154XY) are 0.31 in the X direction, and 0.33 in the Y direction, whereas those of the strengthened model are 0.28 in the X direction, and 0.29 in the Y direction. The decreases of 10% and 12% in the X and Y directions, respectively, were noticed for the strengthened model. The values of seismic coefficients of the strengthened model under MCE (R0.3XY), 0.46 and 0.44 in the X and Y directions, respectively clearly reveal the effect of strengthening, with an increase of strength of more than 50%. Fig. 13 (b) also shows significant increase of base shear strength with the elongation of the fundamental periods in the inelastic response under the more severe earthquakes, R0.4XY. In Fig. 13 (b), the dotted vertical line at 0.156 s represents the estimate of the building period using the empirical equation for the other structures, as defined in KBC 2005 (AIK 2005), and it can be noted that the initial periods of the model are quite similar to this estimate.

Table 5 Test program (X-Taft N21E, Y-Taft S69E)

| Test designation | Intended PGA(g) | | Measured PGA(g) | | Return period in Korea (year) |
|---------------------|-----------------|--------|-----------------|---------------|-------------------------------|
| | X-dir. | Y-dir. | X-dir. | Y-dir. | |
| 0.070 X / R0.070X | 0.07 | - | 0.076 / 0.083 | - | 50 |
| 0.070 XY / R0.070XY | 0.07 | 0.08 | 0.075 / 0.072 | 0.145 / 0.097 | |
| 0.154 X / R0.154X | 0.154 | - | 0.185 / 0.132 | - | 500 |
| 0.154 XY / R0.154XY | 0.154 | 0.177 | 0.210 / 0.123 | 0.289 / 0.186 | |
| 0.187 X / R0.187X | 0.187 | - | 0.209 / 0.174 | - | Design earthquake (DE) |
| 0.187 XY / R0.187XY | 0.187 | 0.215 | 0.268 / 0.147 | 0.284 / 0.220 | |
| / R0.3 X | 0.3 | - | / 0.261 | - | 2400 (MCE) |
| / R0.3 XY | 0.3 | 0.345 | / 0.250 | / 0.374 | |
| / R0.4 X | 0.4 | - | / 0.329 | - | DE in San Francisco, USA |
| / R0.4 XY | 0.4 | 0.46 | / 0.442 | / 0.509 | |

3.3 Global responses

Fig. 14 compares the time histories of responses at the first story of (a) the original model under 0.154XY, and of (b) the strengthened model under R0.187XY. The responses under R0.187XY reveal generally larger torsion moment, while the histories of base shears and deformations became more stable in comparison with those of 0.154XY. Fig. 14 reveals that the time histories of base shear obtained from load cells, V_{LC} , generally match those obtained from the inertia forces, $V_{inertia}$. However, V_{LC} is smaller than $V_{inertia}$ under 0.154XY, while V_{LC} is similar to $V_{inertia}$ under R0.187XY. The levels of base shears and inter-story drifts under 0.154XY and R0.187XY appear to be similar, whereas the overall level of torsional moment and deformation under R0.187XY increased. In Fig 14 (b), the notation “Y2+Y3” in the time history of the base shear means the sum of the base shear in Y2 and Y3 frames, and the “X2” means the base shear in the X2 frame, as given in Fig. 4. These values are very similar to the total base shear in each direction (“Inertial” or “LC”), because X2, Y2, and Y3 frames include walls. The “Frame” in the time history of the overturning moment

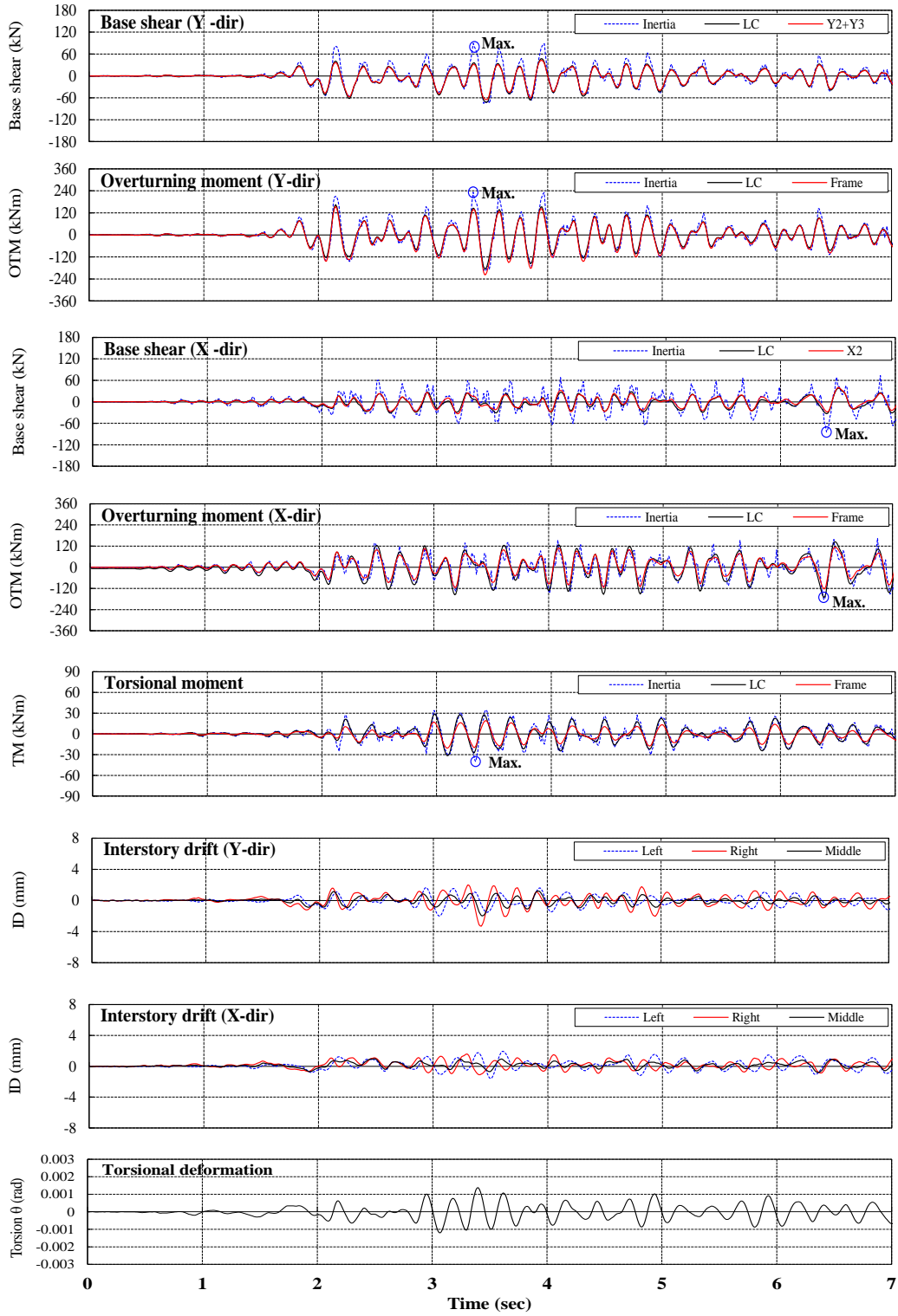


Fig. 14 Time histories of responses at the first story under 0.154XY and R0.187XY: (a) 0.154XY

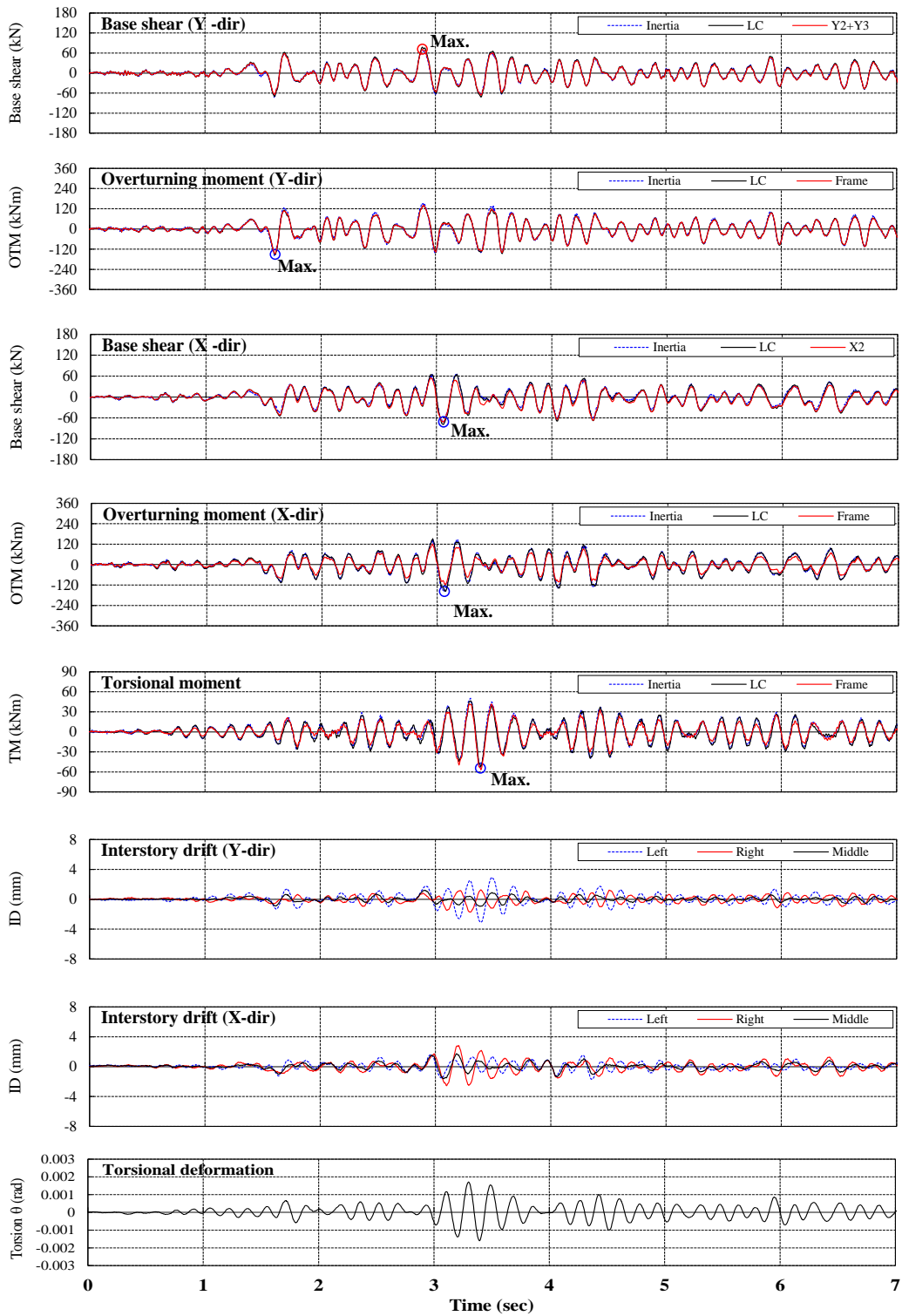


Fig. 14 Time histories of responses at the first story under 0.154XY and R0.187XY: (b) R0.187XY

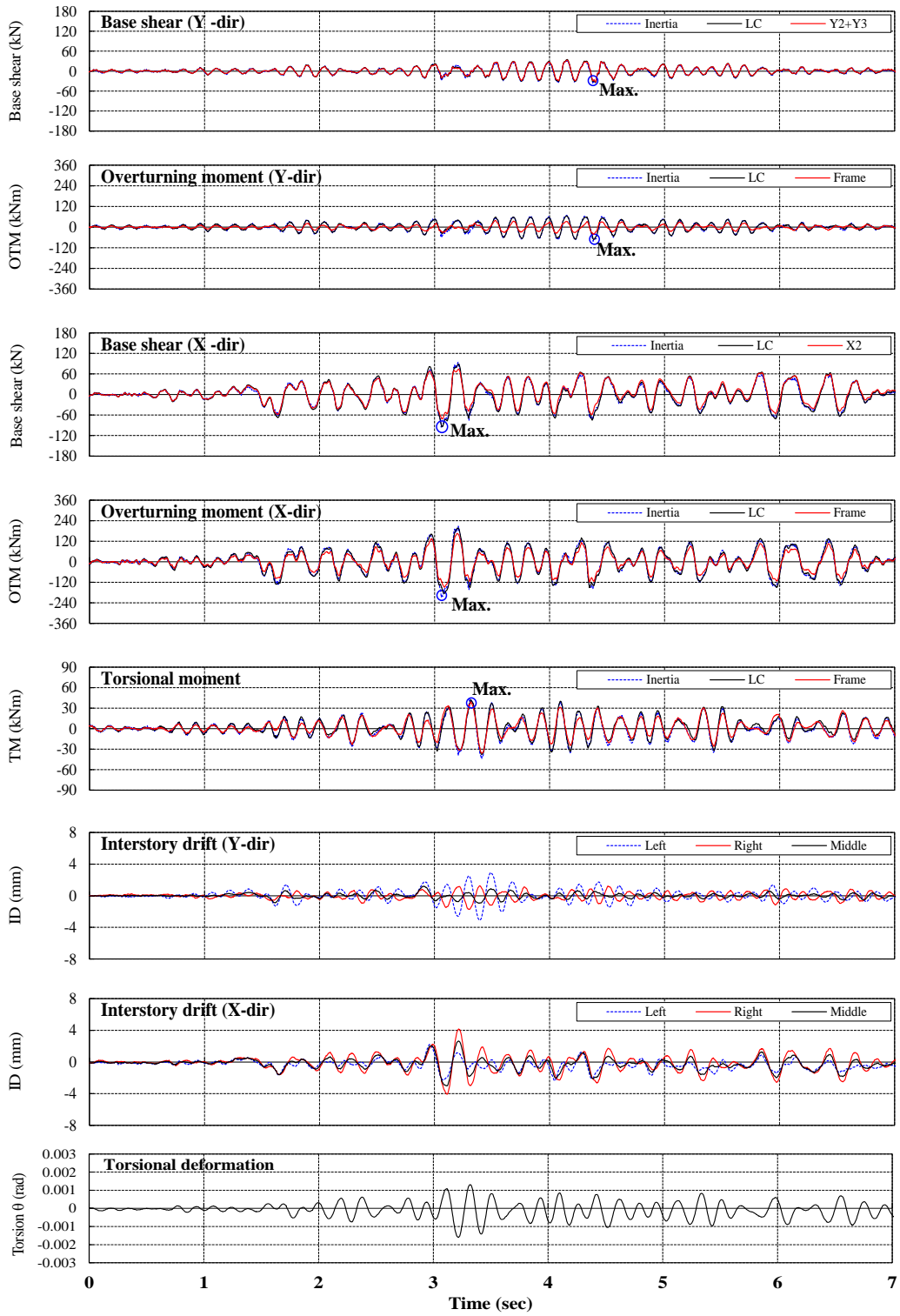


Fig. 15 Time histories of responses at the first story under R0.3X and R0.3XY: (a) R0.3X

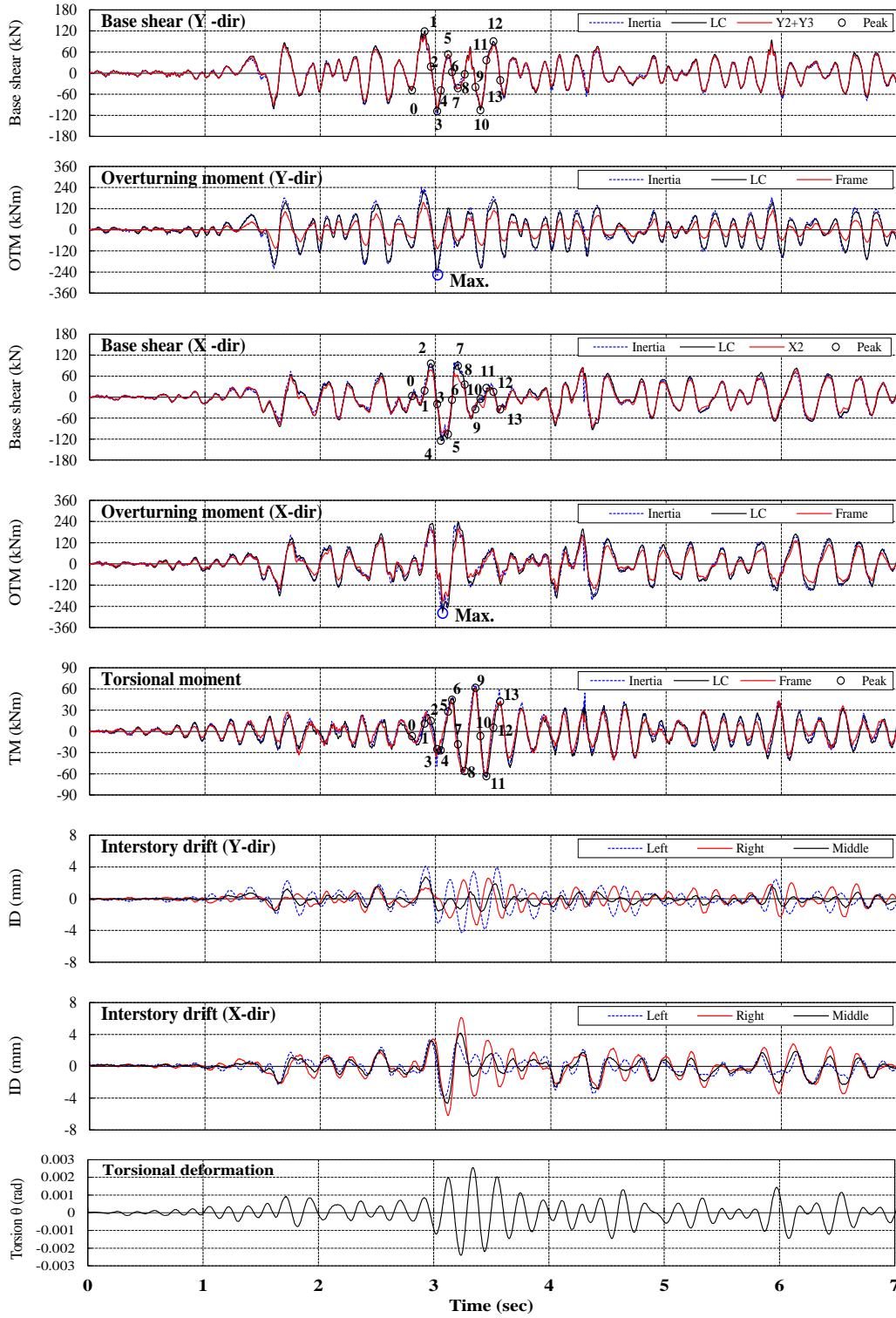


Fig. 15 Time histories of responses at the first story under R0.3X and R0.3XY: (b) R0.3XY

(OTM) means the sum of the OTM contributed by all load cells except LC2, LC3, LC6, and LC7, which constitute the resistance by the stair case walls, and this value occupies a significant portion of the total value of OTM. The resistance ratio of the torsional moment (TM) between the peripheral frames and the wall in the original model was approximately 2:1, but the torsional resistance of the strengthened model was dominated by the peripheral frames. This phenomenon can be easily found at the high level of torsional deformation (TD) during 3~5 seconds, when the history of the TM due to the wall does not follow that of the TM in the peripheral frame.

Fig. 15 compares (a) the responses of the strengthened model under the uni-directional excitations (R0.3X), with (b) those under the bi-directional (R0.3XY) at the level of MCE. In general, the maximum values of responses under R0.3XY appear to be larger than those under R0.3X. In particular, the values of torsion moment, torsion deformation, and interstory drift in the X direction increased significantly. Similar to the test under R0.187XY, the base shears of X2 frame and Y2+Y3 frames under the R0.3XY occupy over 90% of the total base shear in each direction, respectively. Also, most of the overturning and torsion moments are resisted by the peripheral frames.

In Fig. 15 (b), 14 peak points representing peak responses of base shears in X- and Y-directions and torsion moment are given with numeric notations. Numbers 0, 1, 3, 5, 7, 10, and 12 represent peak base shears in the Y direction. Numbers 2, 4, 5, 7, 11 and 13 mean the peak base shears in the X direction; Numbers 6, 8, 9, 11, and 13 show the peak torsion moments. Points 5 and 7 reveal the peak values of base shears in the X and Y directions simultaneously with points 11 and 13, showing the simultaneous peak responses for X-directional shear and torsion moment. There was no peak point that represents the peak responses in the Y-direction shear and torsion moment simultaneously. We will next use these peak points to exploit additional findings, by tracing their hysteretic curves.

Fig. 17 compares the hysteretic behaviors of base shear versus interstory drift ratio (IDR) in the X and Y directions, and torsion moment versus torsion deformation at the first story, under 0.154XY, R0.187XY, R0.3X, and R0.3XY. As shown in Figs. 17 (a) and (b), under the design earthquake (DE), the IDR in the X direction of the strengthened model was 75% larger than that of the original model, while the IDR in the Y-direction of the strengthened model was 39% less than that of the original model. The torsion responses of the strengthened model revealed a slightly larger moment and deformation than those of the original model. The relation between shear force and drift in the X direction under R0.187XY shows significant energy dissipation through the inelastic behavior, in comparison to the minimal energy dissipation of the original model under

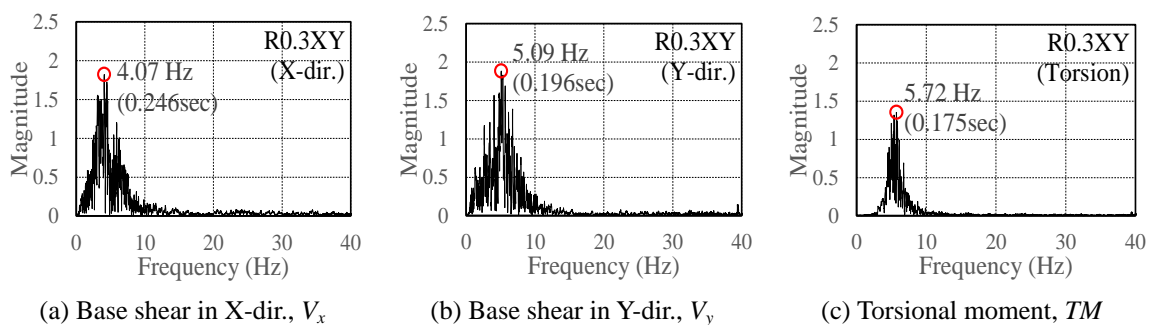


Fig. 16 FFT plot by using the time histories of base shear and torsional moment under R0.3XY (Fig. 15)

0.154XY. The values of the lateral stiffness in the X and Y directions under 0.154XY were equal to 57kN/mm, and these values under R0.187XY were 57 kN/mm and 80kN/mm, respectively. The value of torsional stiffness of the original model was about 30MN/rad under 0.154XY. But, it can be found that the torsional stiffness of the strengthened model has dual values of stiffness, 30MNm/rad at the high level and 50MNm/rad at the low level of excitations. This variation of the torsional stiffness results from the wall behavior. As shown in Figs. 14 and 15, the time history of torsional moment resisted by the walls did not contribute to the maximum torsional moment during the 3~3.8 second time period, though the walls resisted most of the base shear.

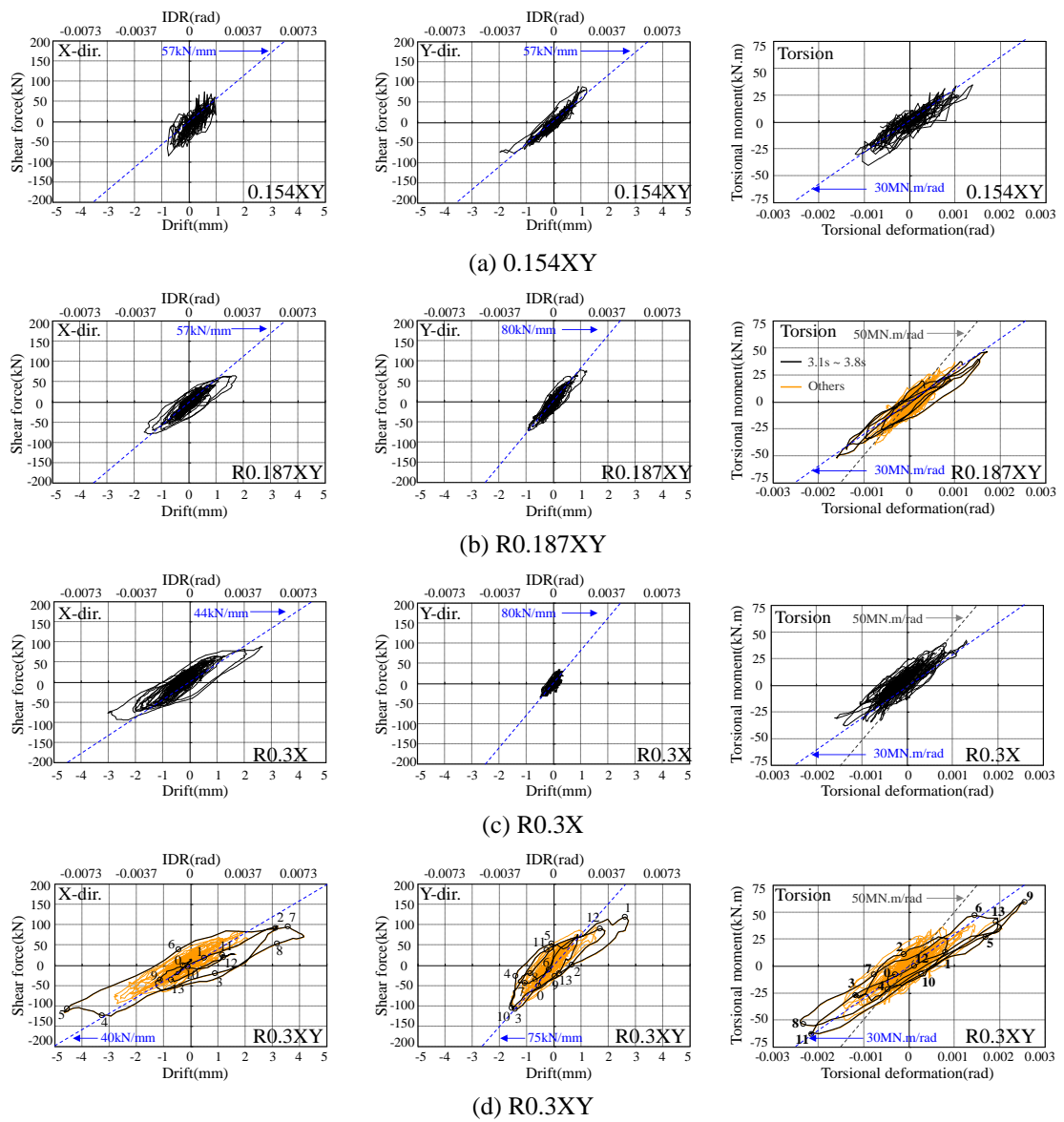


Fig. 17 Interstory drift vs. base shear (LC) and torsional deformation vs. torsional moment (LC)

As shown in Figs. 17 (c) and (d), IDR in the X direction and torsional deformation under the bi-directional excitation, R0.3XY, were approximately 50% and 60% larger than those under the uni-directional excitation, R0.3X, respectively. R0.3XY induced significantly increased inelasticity with larger energy dissipation, when compared with minor inelastic responses under R0.187XY. For the strengthened model, the stiffness degradation can be noticed in Fig. 17, as the intensity of excitation increased. When the peak points denoted in Fig. 15 for R0.3XY are plotted in the hysteretic curves in Fig. 17 (d), it can be found that the largest energy dissipation through the inelastic behavior occurred in the range of peak points 2 to 9 in the X directional translation, in the range of peak points 0 to 5 in the Y directional translation, and in the range of peak points 1 to 13 in the torsion in the counterclockwise direction. These peak values during the large energy dissipation occurred at different instants of time.

Fast Fourier Transform (FFT) was applied to the time histories of base shear and torsion moment for each test as such the case of test R0.3XY in Fig. 16, and the obtained periods are given in Table 6. The first mode of the original model is the torsion mode ($T = 0.248\text{s}$), and the second mode is the translational mode in the Y direction ($T = 0.219\text{s}$), with the third mode being the translational mode in the X direction ($T = 0.160\text{s}$) under 0.154XY. Although the primary mode of the strengthened model was still the torsional mode ($T = 0.163\text{s}$) under R0.154XY, and the primary mode was changed from the torsional mode ($T = 0.175\text{s}$) to the translation mode in the X direction ($T = 0.246\text{s}$), after the MCE (R0.3XY). As shown in Fig. 13 (b), the estimate of the building period using the empirical equation for the other structures, as defined in KBC 2005 (AIK 2005), 0.156 s, appears to be reasonable, in comparison to these obtained periods.

Fig. 18 shows the possible regression curves between the maximum base shear (or base torsion) and IDR at the ground story (or base torsion angle). The rectangular marks denote the maximum base shear and the corresponding IDR whereas the circular marks represent the maximum IDR and corresponding base shear. Also, the hollow marks represent the results of the original model with the solid marks showing the case of the strengthened model. Figs. 18 (a) and (b) compare the relation of base shear and IDR at the first story in the X and Y direction, respectively, and nonlinear behavior can be found after R0.154XY and R0.187XY. The yielding IDR in the X and Y direction are 0.296% and 0.185%, respectively. Under R0.4XY, the IDR in the negative X direction is 1.54%, which exceeded the limit of 1.5% allowed in the KBC 2005. In Fig. 18(b), the reason for the directional bias in the responses is considered to be due to the asymmetrical plan in the Y direction. The IDR and the base shear became larger when the wall is subjected to tension forces (+). Fig. 18 (c) shows the relation between the torsion moment (TM) and the torsion deformation (TD) at the first story. The slope drastically decreases after R0.154XY and R0.187XY. The yield angle (θ_y) of the TD was estimated to be 0.0018rad.

Table 6 Natural periods (unit: sec)

| Test | Original model | | | Strengthened model | | | | |
|----------------|----------------|---------|---------|--------------------|----------|----------|--------|--------|
| | 0.07XY | 0.154XY | 0.187XY | R0.07XY | R0.154XY | R0.187XY | R0.3XY | R0.4XY |
| V_x | 0.160 | 0.160 | 0.160 | 0.160 | 0.160 | 0.160 | 0.246 | 0.324 |
| FFT V_y | 0.202 | 0.219 | 0.214 | 0.160 | 0.149 | 0.196 | 0.196 | 0.247 |
| <i>Torsion</i> | 0.248 | 0.248 | 0.248 | 0.160 | 0.163 | 0.163 | 0.175 | 0.223 |

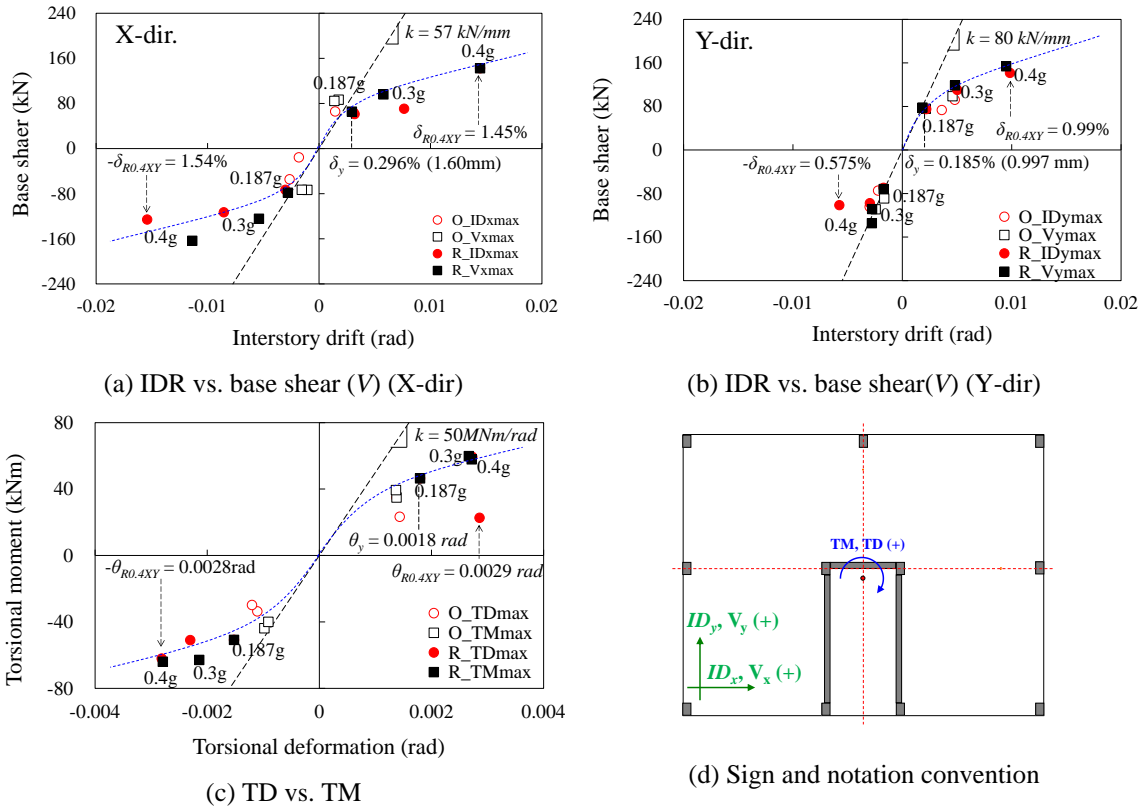


Fig. 18 Relation between the maximum responses and corresponding deformations (O: derived from inertia forces of original model, R: obtained from load cells of strengthened model)

3.4 Comparison of stiffness and strength of frames between design and test results

Fig. 19 shows the hysteretic relation of force and drift in frames under R0.3XY (MCE), and Table 7 compares the yield displacement, strength, and stiffness of each frame of the design and the test results. The curves of the peripheral frames, X3, Y1, and Y4, represent nearly elastic behaviors, while those of the inner walls (X2, Y2, and Y3) show inelastic behavior. The values of stiffness and strength of the experiment under R0.3XY were generally much lower than those of the design. In the case of frame X3 strengthened with BRB's, the stiffness and strength of the experiment were 4.07kN/mm and 12.7kN, respectively, whereas those of the design were 34.5kN/mm and 40.8kN, respectively. Although the peripheral frames, X3, Y1, and Y4, were strengthened by the BRB's, the values of stiffness of these frames (X3: 4.07kN/mm, Y1: 4.26kN/mm, Y4: 4.69kN/mm) were similar to that of X1 frame, 4.04kN/mm, which was not strengthened.

In the sub-assembly test of specimen LC1, which has the identical boundary condition with the earthquake simulation test, the values of yield drift and the stiffness of LC1 were 5.1mm and 6.0kN/mm (Table 4), respectively. In the earthquake simulation test, the maximum drift of the strengthened frame, 3.35mm, was smaller than 5.1mm, which means that the BRB's remained in

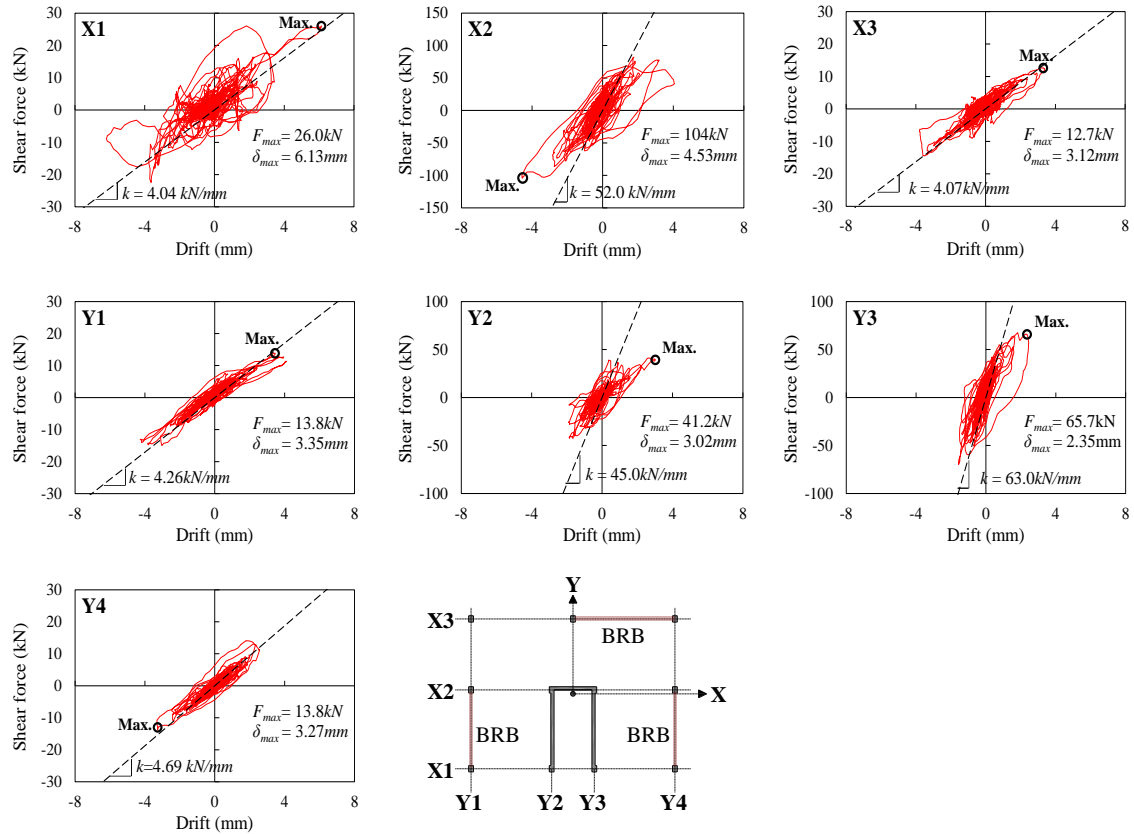


Fig. 19 Relation of force versus drift in frames under R0.3XY (MCE)

Table 7 Comparison of stiffness and strength between design and test results of strengthened model

| Frame (S: Strengthened with BRB) | Prototype (design, Fig.6) | | | 1:5 scale model (design) | | | R0.3XY (test) | | |
|--|---------------------------|---------------|--------------------------|--------------------------|---------------|--------------------------|------------------------|-------------------|-------------------------|
| | δ_y (mm) | F_y (kN) | $k_{elastic}$ (kN/mm) | δ_y (mm) | F_y (kN) | $k_{elastic}$ (kN/mm) | δ_{Max} (mm) | F_{Max} (kN) | $k_{R0.3XY}$ (kN/mm) |
| X1 | 11.54 | 368 | 31.9 | 2.31 | 14.72 | 6.4 | 6.13 | 26.0 | 4.04 |
| X2 | 4.27 | 1400 | 328.4 | 0.85 | 56.0 | 65.7 | 4.53 | 104 | 52.0 |
| X3 (S) | 5.89 | 1020 | 172.4 | 1.18 | 40.8 | 34.5 | 3.12 | 12.7 | 4.07 |
| Y1 (S) | 7.42 | 1130 | 152.4 | 1.48 | 45.2 | 30.5 | 3.35 | 13.8 | 4.26 |
| Y2 | 3.41 | 2030 | 595.0 | 0.68 | 81.2 | 119.0 | 3.02 | 41.2 | 45.0 |
| Y3 | 3.41 | 2030 | 595.0 | 0.68 | 81.2 | 119.0 | 2.35 | 65.7 | 63.0 |
| Y4 (S) | 13.3 | 1130 | 152.4 | 2.66 | 45.2 | 30.5 | 3.27 | 13.8 | 4.69 |

the elastic range. The values of stiffness of the strengthened frames were 4.34kN/mm on average, which is similar to the result of the static sub-assembly test, 6.0kN/mm. Therefore, the BRB's have just functioned in earthquake simulation tests as ordinary braces rather than being BRB's,

because their design stiffness was not obtained, due to the large deformation at the joint between the frame and BRB's, and the foundation flexibility. The rigidity of connections between the existing concrete member and the BRB's, and the rigidity of columns in tension and the foundation should be investigated systematically in the future to ensure the successful application of BRB's to the existing RC building structures.

3.5 Lateral resistance of the X-directional wall

Fig. 20 shows the bias to the tension side, in the time history of axial force obtained from load cells LC6 and LC7 in Fig. 12 (d) in the wall unique in the X direction under 0.154XY, when compared with the case of 0.154X. The reason for this bias in the tension side under 0.154XY is

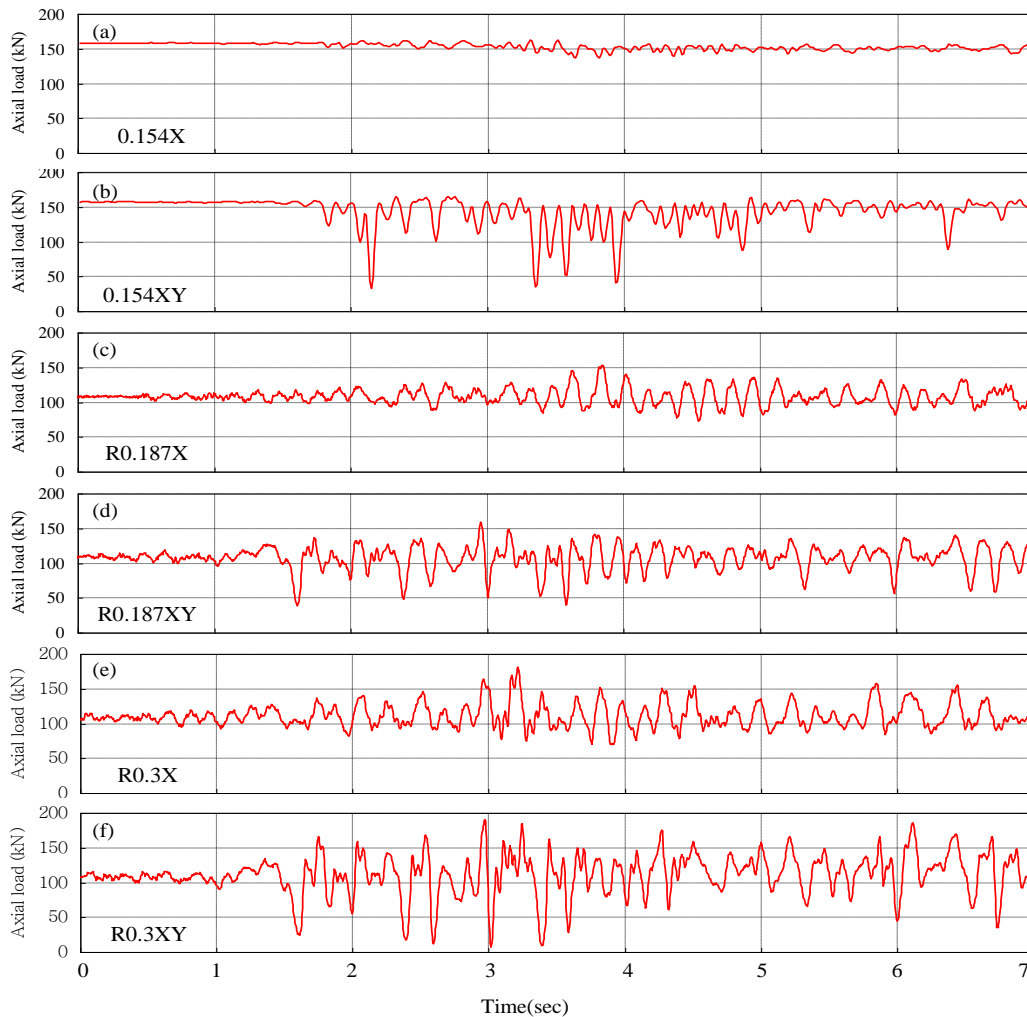


Fig. 20 Time histories of axial force of wall C6-C7 (X direction wall)
 (a) 0.154X, (b) 0.154XY, (c) R0.187X, (d) R0.187XY, (e) R0.3X, and (f) R0.3XY

due to the rocking phenomenon in the Y direction caused by the Y-directional excitations. This bias, however, decreased in the response of the strengthened model under R0.187XY and R0.3XY. In contrast, it is interesting to note that the strengthened model revealed the tendency of bias to axial compressive force in the wall, regardless of the uni- or bi-directional excitations. The reason for this phenomenon is considered to be the elongation of the wall caused by lateral movement, and the constraint to this elongation provided by the peripheral BRB frames, which were absent in the original model. This reasoning is justified in Fig. 21, where the hysteretic curves between the axial force and the bending moments obtained from load cells LC6 and LC7 in Fig. 12 (d) are plotted with the P-M interaction capacity diagram. The strengthened model showed the increase of the compressive axial force with the increase of the bending moment in Figs. 21 (b), (c), and (d), whereas the original model revealed the decrease of the compressive axial force with the increase of the bending moment in Fig. 21 (a).

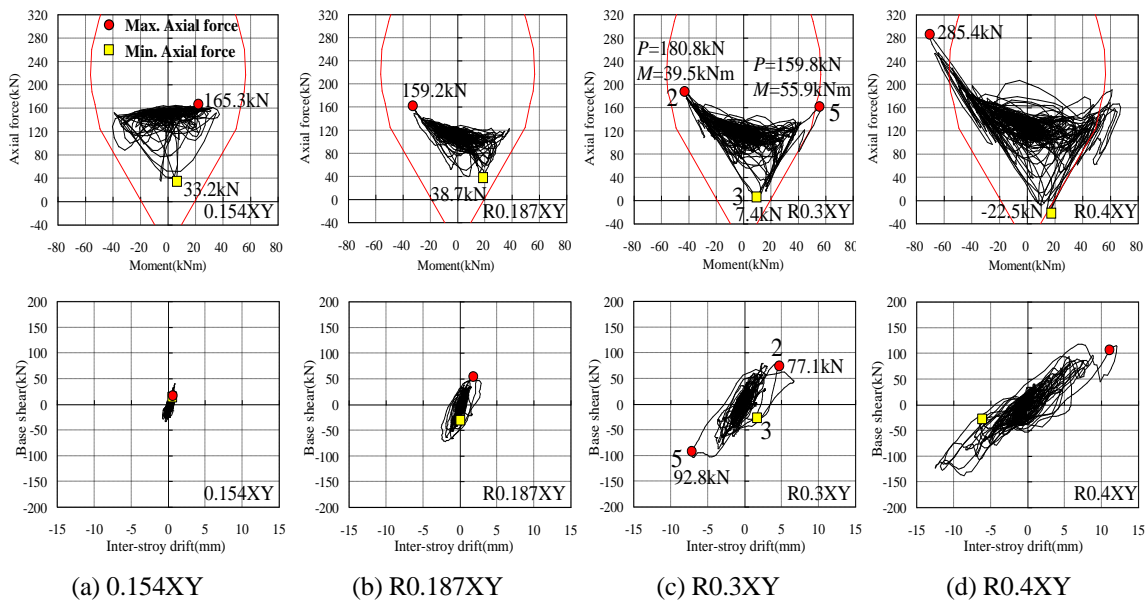


Fig. 21 P-M interaction diagram and relation of base shear versus drift in wall C6-C7

The increase of the axial compressive force again means the increase of the bending moment capacity, which leads to significant increase in the lateral resistance of the wall, as identified in the hysteretic curves between the base shear and the first-story drift in the wall in Fig. 21. The ultimate lateral strength of the wall can be estimated using the bending moment distribution assumed in Fig. 22. For example, the hysteretic curve reaches the P-M interaction diagram with the ultimate bending moment being $M_p = 55.9\text{kNm}$ at point 5 in Fig. 21 (c). With the application of this value to the assumed relationship between the bending moment and the shear force in Fig. 22, the shear resistance, $V_p = 1.0 \cdot (55.9\text{kN}) / 0.54\text{m} = 104\text{kN}$, can be estimated, which is comparable to the experimental result, $V_p = 92.8\text{kN}$ at point 5. This strength is approximately two times higher than the nominal shear strength of the wall, 56.0kN , as given in Table 7. Also, it can be found in Fig. 21 (c) that the lowest compressive force at point 3 in the hysteretic curve of P-M interaction induced the

significant reduction of the lateral stiffness at point 3 in the corresponding hysteretic curve of shear force versus lateral drift.

The final crack patterns in the walls, C2-C6, C6-C7, and C3-C7 are shown in Fig. 23. Serious shear cracks occurred under R0.3X and R0.3XY in wall C6-C7, and these cracks were aggravated under R0.4XY, with the residual crack width being approximately 0.3mm.

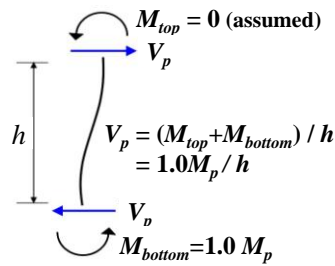


Fig. 22 Shear and bending moments in wall C6-C7

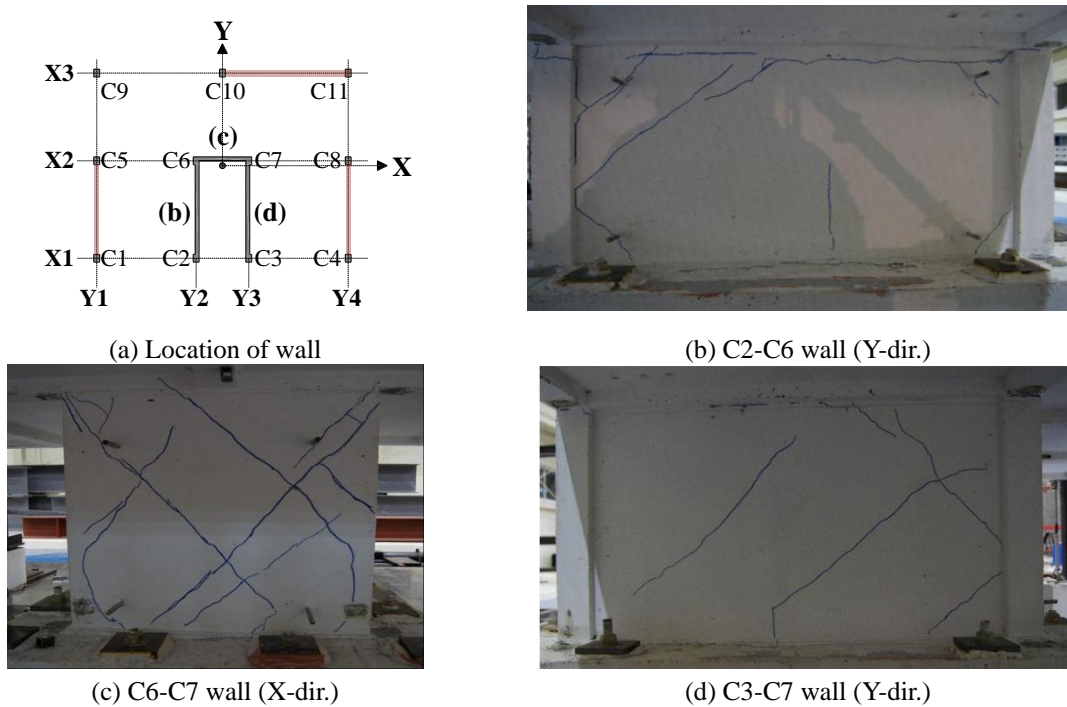


Fig. 23 Crack patterns after R0.4XY

3.6 Resistance mechanisms of base shear and overturning moment

Fig. 24 shows the distribution of the base shear at the maximum response under R0.3XY, in which the base shear is concentrated at the bottom of the walls. In Table 8, the contributions of

walls in the X and Y direction appear to be more than 80% of the total base shear at the instant of the maximum base shear, under 0.154XY, 0.187XY, R0.187XY, and R0.3XY. The design concept of the strengthened model was that the contributions of the frame and the wall were similar each other. However, the contributions of the frame in the strengthened model appear to be less than 20% of the total base shear, due to the slip at the joint between the frame and the BRB's, and the foundation flexibility.

Fig. 25 shows the distributions of the axial forces in the load cells at the maximum response under R0.3XY. In Table 9, the OTM resistance ratios of the peripheral frame in the X and Y direction at the maximum response under R0.187XY and R0.3XY were more than approximately 80% and 50% of the total OTM, respectively. Because the load cells under the columns of C1, C2, and C3 in the original model were in error, the OTM of the original and strengthened model could not be compared.

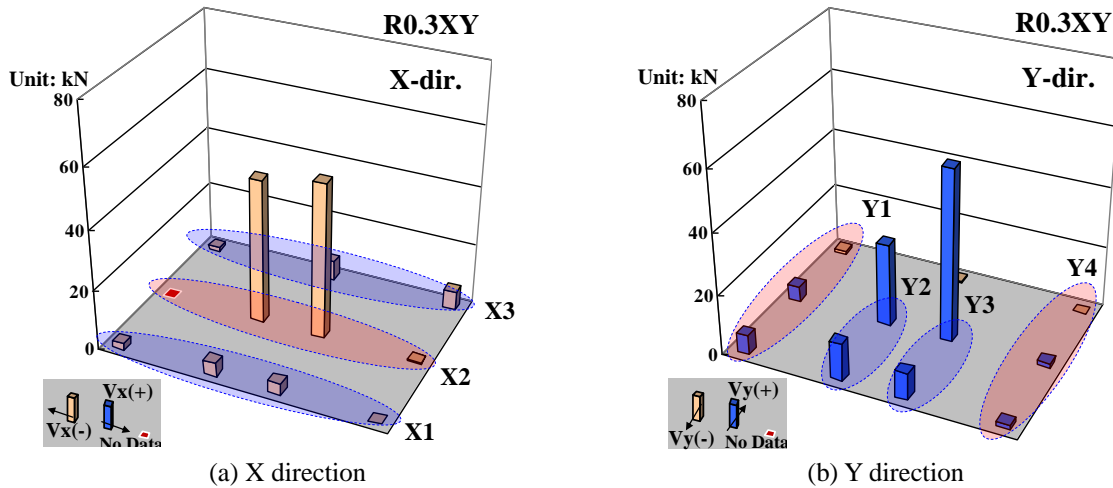


Fig. 24 Base shear distribution in the load cells at the instant of max. base shear (R0.3XY)

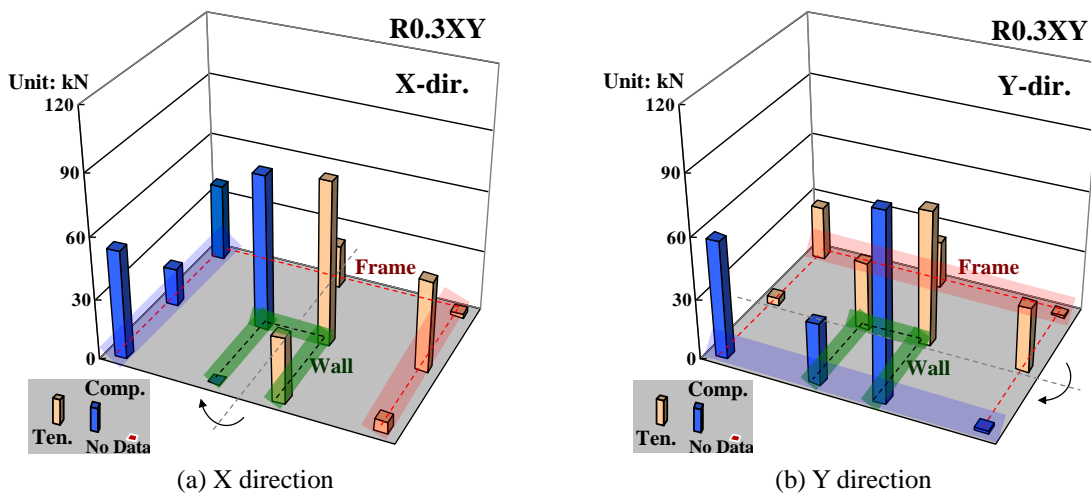


Fig. 25 Axial force distribution in the load cells at instant of max. OTM (R0.3XY)

Table 8 Distributions of base shear

| Test | | Max. Base shear (kN) | | | | | |
|----------|-----|----------------------|--------------|-------|------------------|-----------------|-------|
| | | X-dir. | | | Y-dir. | | |
| | | Frame (X1+X3) | Wall (X2) | Total | Frame (Y1+Y4) | Wall (Y2+Y3) | Total |
| 0.154XY | kN% | -1.6 | 39.9 | 38.3 | 7.0 | 65.1 | 72.1 |
| | | -4 | 104 | 100 | 10 | 90 | 100 |
| R0.187XY | kN% | 7.8 | 70.8 | 78.6 | 6.2 | 71.6 | 77.8 |
| | | 10 | 90 | 100 | 8 | 92 | 100 |
| R0.3XY | kN% | 25.2 | 99.5 | 124.7 | 13.0 | 105.6 | 118.6 |
| | | 20 | 80 | 100 | 11 | 89 | 100 |

Table 9 Distributions of OTM

| Test | | Max. OTM (kNm) | | | | | |
|----------|----|----------------|------|-------|--------|-------|-------|
| | | X-dir. | | | Y-dir. | | |
| | | Frame | Wall | Total | Frame | Wall | Total |
| R0.187XY | kN | 121.7 | 30.8 | 152.5 | 71.6 | 74.7 | 146.3 |
| | % | 80 | 20 | 100 | 49 | 51 | 100 |
| R0.3XY | kN | 212.0 | 51.7 | 263.7 | 107.8 | 120.8 | 228.6 |
| | % | 80 | 20 | 100 | 47 | 53 | 100 |

4. Conclusions

In a 1:5 scale model of a low-rise RC apartment building having a high degree of irregularity regarding the weak/soft story and torsion at the ground story, the ground-story columns were strengthened with FRP sheets, to avoid brittle collapse due to shear failure followed by axial compression failure, and the outer frames at the ground story were infilled with BRB's, to increase the stiffness, strength, and energy dissipation capacity within the allowed range of lateral drift. To verify the effectiveness of this strengthening, a series of earthquake simulation tests were conducted before and after the strengthening, and these test results are compared and analyzed, to check the effectiveness of the strengthening. Based on these investigations, the following conclusions are made:

(1) The concept of Buckling Restrained Braces (BRB's) is to use an inner core artificially designed to yield prematurely in compression and tension, enclosed by strong buckling restraining braces, thereby to dissipate large seismic input energy, within the allowed range of displacement. This concept has attracted wide interest, and has been applied to many new constructions and the seismic retrofitting of existing steel structures. However, despite this advantage in concept, there have been many problems to be solved in the detailed design, such as joints with connected members. The study conducted herein again revealed the detail problems in adoption of BRB's into the existing RC frames: The BRB's showed significant slippage at the joint with the existing RC beam, up-lift of columns from RC foundations, foundation deformation due to the flexibility of the foundation itself, all of which finally led to failure, due to the buckling of base joint angles. Because of these factors, the value of lateral stiffness of the RC frame strengthened with BRB's and FRP sheets appeared to be as low as one seventh of the intended value. This low stiffness led

to a large yield displacement, and therefore the BRB's could not dissipate seismic input energy as desired within the range of anticipated displacement. The rigidity of connections between the existing concrete member and the BRB's, and the rigidity of columns in tension and the foundation should be investigated systematically in the future to ensure the successful application of BRB's to the existing RC building structures.

(2) Although, the strengthened model did not behave as desired, it showed great enhancement in earthquake resistance, not only under the maximum considered earthquake in a low-to-moderate seismicity region, such as Korea, but also under the intensity level of design earthquake in a strong seismic region, such as San Francisco. The followings are some important seismic behaviors of the strengthened model, which have contributed to this enhanced earthquake resistance:

- The strengthened model revealed the tendency of bias towards axial compression in the wall, regardless of the uni- or bi- directional excitation. The reason is considered to be elongation of the wall caused by lateral drift, and the constraint to this elongation provided by the peripheral BRB frames, which were absent in the original model. This increase of the axial compressive force in the walls means an increase of the bending moment capacity, which leads to a significant (approximately 50%) increase in the lateral resistance of the wall.
- The inner core walls resisted over 90% of the maximum base shear, while the peripheral frames took charge of more than 50% of the OTM. Base torsion was resisted by both the inner core wall, and the peripheral frames in the original model, up to the design earthquake in Korea (0.154XY). In contrast, the strengthened model resisted most of the base torsion with the peripheral frames, after yielding of the inner core walls. The model represented dual values of stiffness, of 50MN/rad when the core walls did not yield, and 30MN/rad when the core wall did yield.
- Whereas the fundamental mode of the original and strengthened model remains the torsional mode, the periods of the second and third translational modes became very close to the fundamental mode in case of the strengthened model. But, when the strengthened model was subject to severe earthquake ground excitations (R0.3XY), it had a translation mode in the X-direction as the fundamental mode.
- The strengthened model had the curve of base shear versus story drift at the first story that showed the first significant yielding under design earthquake (R0.187XY), and inelastic behavior with large energy dissipation under the maximum considered earthquake (R0.3XY). However, the maximum IDR's for R0.187XY and R0.3XY in the X direction were 0.296% and 0.854%, respectively, which were within the allowable limit of 1.5% for the limit state of life safety.

The design implications learned through this experimental study, such as overstrength factor, torsion eccentricity, and bi-directional effect, will be presented in a separate paper, due to the length limitation of this paper.

Acknowledgments

The research presented herein was supported by the National Research Foundation of Korea, through the contracts NRF-2007-0054740 and NRF-2009-0078771. The writers are grateful for this support.

References

- ACI Committee 318 (2005), *Building code requirements for structural concrete and commentary* (ACI 318-05), American Concrete Institute, Detroit.
- Architectural Institute of Korea (2005), *Korean building code* (KBC2005), Seoul, Korea. (in Korean)
- Chen, C.C. (2002), "Recent advances of seismic design of steel buildings In Taiwan, International Training Programs for Seismic Design of Building Structures", National Center for Research on Earthquake Engineering, Republic of China, 105-123.
- Chou, C.C. and Chen, P.J. (2009), "Compressive behavior of central gusset plate connections for a buckling-restrained brace frame", *J. Constr. Steel Res.*, **65**(5), 1138-1148.
- Chou, C.C. and Liu, J.H. (2012), "Frame and brace action forces on steel corner gusset plate connections in buckling-restrained braced frames", *Earthq. Spectra*, **28**(2), 531-551.
- Chou, C.C., Liu, J.H. and Pham, D.H. (2012), "Steel buckling-restrained braced frames with single and dual corner gusset connections: seismic tests and analyses", *Earthq. Eng. Struct. Dyn.*, **41**(7), 1137-1156.
- De Witte, F.C. and Kikstra, W.P. (2005), *DIANA – Finite element analysis*, TNO DIANA BV.
- Fukuta, T., Kabeyasawa, T., Kuramoto, H. and Sanada, Y. (2001), "Shaking table tests and design analysis of a wall frame structure with soft first story", *4th international symposium on earthquake engineering for the moderate seismicity regions*, Seoul, Korea, 94-112.
- International Code Council (2000), *International building code*, Falls church, VA.
- Erochko, J., Christopoulos, C., Tremblay, R. and Choi, H. (2011) "Residual drift response of SMRFs and BRB frames in steel buildings designed according to ASCE 7-05", *J. Struct. Eng.*, **137**(5), 589-599.
- Khampanit, A., Chatree, N., Surasak, N., Sutat, L. and Pennung, W. (2011), "Cyclic testing of a non-ductile reinforced concrete frame strengthened with buckling restrained brace", *The 2011 World Congress on Advances in Structural Engineering and Mechanics*, Seoul, Korea, 1900-1909.
- Lee, H.S., Jung, D.W., Lee, K.B., Kim, H.C. and Lee, K. (2011a), "Shake-table responses of a low-rise RC building model having irregularities at first story", *Struct. Eng. Mech.*, **40**(4), 517-539.
- Lee, H.S., Lee, K.B., Hwang, S.J. and Cho, C.S. (2011b), "Reversed lateral load tests on RC frames retrofitted with BRB and FRP", *J. Korea Concrete Inst.*, **23**(5), 683-692. (in Korean)
- Priestley, M.J.N. and Seible, F. (1995), "Design of seismic retrofit measures for concrete and masonry structures", *Constr. Build.Mater.*, **9**(6), 365-377.
- Sheikh, S.A. and Li, Y. (2007), "Design of FRP confinement for square concrete column", *Eng. Struct.*, **29**(6), 1074-1083.
- Teng, J.G., Chen, J.F., Smith, S.T. and Lam, L. (2002), *FRP-strengthened RC Structures*, John Wiley & Sons, LTD.
- Teran-Gilmore., A. and Vitro-Cambray, N. (2009), "Preliminary design of low-rise buildings stiffened with buckling-restrained brace by a displacement-based approach, Earthquake Spectra", *Earthq. Eng. Res. Inst.*, **25**(1), 185-211.
- Tremblay, R., Degrange, G. and Blouin, J. (1999), "Seismic rehabilitation of a four-storey building with a stiffened bracing system", *Proc. 8th Canadian Conference on Earthquake Engineering*, Vancouver, B.C., 549-554.
- Zhao, B., Taucer, F. and Rossetto, T. (2009), "Field investigation on the performance of building structures during the 12 May 2008 Wenchuan earthquake in China", *Eng. Struct.*, **31**(8), 1707-1723.